Origin of Tight Binding of a Near-Perfect Transition-State Analogue by Cytidine Deaminase: Implications for Enzyme Catalysis

Haobo Guo, Niny Rao, Qin Xu, and Hong Guo*

Contribution from the Department of Biochemistry and Cellular and Molecular Biology, Center of Excellence in Structural Biology, University of Tennessee, Knoxville, Tennessee 37996-0840

Received October 4, 2004; E-mail: hguo1@utk.edu

Abstract: Cytidine deaminase (CDA) is a zinc metalloenzyme that catalyzes the hydrolytic deamination of cytidine to uridine. Zebularine (ZEB) binds to CDA, and the binding process leads to a near-perfect transition-state analogue (TSA) inhibitor at the active site with an estimated K_i value of 1.2×10^{-12} M. The interaction of CDA with the TSA inhibitor has become a paradigm for studying the tight TSA binding by enzymes. The formation of the TSA is catalyzed by CDA by a mechanism that is similar to the formation of the tetrahedral intermediate during the CDA-catalyzed reaction (i.e., through the nucleophilic attack of a Zn−hydroxide group on C_4). It is believed that the TSA formed at the active site is zebularine 3,4-hydrate. In this paper, it is shown from QM/MM molecular dynamics and free energy simulations that zebularine 3,4-hydrate may in fact be unstable in the enzyme and that a proton transfer from the Zn−hydroxide group to Glu-104 during the nucleophilic attack could be responsible for the very high affinity. The nucleophilic attack by the Zn−hydroxide on C_4 is found to be concerted with two proton transfers. Such concerted process allows the TSA, an alkoxide-like inhibitor, to be stabilized through a mechanism that is similar to the transition-state stabilization in the general acid−base catalysis. It is suggested that the proton transfer from the Zn−hydroxide to Glu-104, which is required to generate the general acid for protonating the leaving ammonia, may play an important role in lowering the activation barrier during the catalysis.

Introduction

Enzymes' catalytic power lies in their ability to stabilize transition state (TS) and to lower the energy barriers for enzyme-catalyzed reactions. It has been recognized that a molecule that mimics the altered structure of substrate in the transition state may capture a significant fraction of transition-state stabilization and can therefore bind to the enzyme tightly.[1−8] The precise arrangements of many transition-state analogue (TSA) inhibitors in enzyme active sites have been determined by X-ray crystallography.[9,10] These structures have led to significant insights into the interactions that might be responsible for transition-state stabilization. The transition-state analogue approach has been very useful for the design of potent inhibitors and is critical for the generation of catalytic antibodies. Nevertheless, many questions remain concerning the details of TSA binding and the energetic origin of the high binding affinities, including the role of proton transfers.

In this paper, quantum mechanical/molecular mechanical (QM/MM) molecular dynamics simulations are performed for *Escherichia coli* cytidine deaminase (CDA)[11] to study the mechanism of inhibitor binding and the energetic origin of the high binding affinity for a near-perfect TSA inhibitor. CDA catalyzes the hydrolytic deamination of cytidine to uridine (Figure 1A) and has been a subject of extensive investigations.[11−25]

(1) Wolfenden, R. *Nature* **1969**, *223*, 704−705.
(2) Wolfenden, R. *Acc. Chem. Res.* **1972**, *5*, 10−18.
(3) Wolfenden, R.; Kati, W. M. *Acc. Chem. Res.* **1991**, *24*, 209−215.
(4) Wolfenden, R. *Annu. Rev. Biophys. Bioeng.* **1976**, *5*, 271−306.
(5) Radzicka, A.; Wolfenden, R. *Methods Enzymol.* **1995**, *249*, 284.
(6) Schramm, V. L. *Annu. Rev. Biochem.* **1998**, *67*, 693−720.
(7) Morrison, J. F.; Walsh, C. T. *Adv. Enzymol. Relat. Area Mol. Biol.* **1988**, *61*, 201−301.
(8) Mader, M. M.; Bartlett, P. A. *Chem. Rev.* **1997**, *97*, 1281−1301.
(9) Lolis, E.; Petsko, G. A. *Annu. Rev. Biochem.* **1990**, *59*, 597−630.
(10) Lipscomb, W. N.; Strater, N. *Chem. Rev.* **1996**, *96*, 2375−2433.

(11) Xiang, S.; Short, S. A.; Wolfenden, R.; Carter, C. W., Jr. *Biochemistry* **1995**, *34*, 4516−4523.
(12) Betts, L.; Xiang, S.; Short, S. A.; Wolfenden, R.; Carter, C. W., Jr. *J. Mol. Biol.* **1994**, *235*, 635−656.
(13) Carlow, D. C.; Short, S. A.; Wolfenden, R. *Biochemistry* **1996**, *35*, 948−954.
(14) Carlow, D. C.; Smith, A. A.; Yang, C. C.; Short, S. A.; Wolfenden, R. *Biochemistry* **1995**, *34*, 4220−4224.
(15) Smith, A. A.; Carlow, D. C.; Wolfenden, R.; Short, S. A. *Biochemistry* **1994**, *33*, 6468−6474.
(16) Snider, M. J.; Gaunitz, S.; Ridgway, C.; Short, S. A.; Wolfenden, R. *Biochemistry* **2000**, *39*, 9746−9753.
(17) Xiang, S.; Short, S. A.; Wolfenden, R.; Carter, C. W., Jr. *Biochemistry* **1996**, *35*, 1335−1341.
(18) Xiang, S.; Short, S. A.; Wolfenden, R.; Carter, C. W., Jr. *Biochemistry* **1997**, *36*, 4768−4774.
(19) Snider, M. J.; Wolfenden, R. *Biochemistry* **2001**, *40*, 11364−11371.
(20) Lewis, J. P.; Carter, C. W., Jr.; Hermans, J.; Pan, W.; Lee, T.-S.; Yang, W. *J. Am. Chem. Soc.* **1998**, *120*, 5407−5410.
(21) Lewis, J. P.; Liu, S.; Lee, T.-S.; Yang, W. *J. Comput. Phys.* **1999**, *151*, 242−263.
(22) Frick, L.; MacNeela, J. P.; Wolfenden, R. *Bioorg. Chem.* **1987**, *15*, 100−108.
(23) Xu, Q.; Guo, H. *J. Phys. Chem. B* **2004**, *108*, 2477−2483.
(24) Frick, L.; Yang, C.; Marquez, V. E.; Wolfenden, R. *Biochemistry* **1989**, *28*, 9423−9430.
(25) Snider, M. J.; Reinhardt, L.; Wolfenden, R.; Cleland, W. W. *Biochemistry* **2002**, *41*, 415−421.
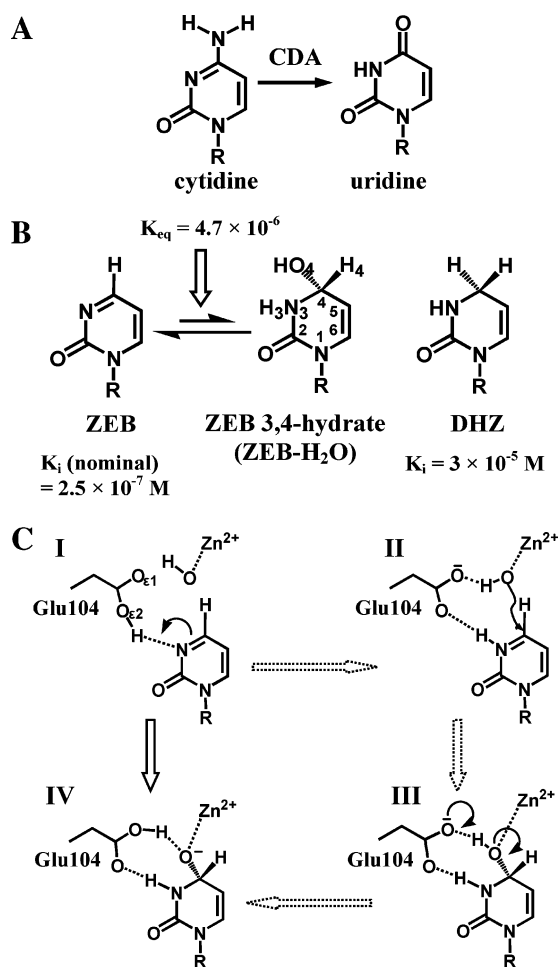
Figure 1. (A) Hydrolytic deamination of cytidine to uridine catalyzed by cytidine deaminase (CDA); R = ribose. (B) Pyrimidin-2-one ribonucleoside (zebularine or ZEB), zebularine 3,4-hydrate (ZEB−H_2O), and 3,4-dihydro-zebularine (DHZ). Subscripts are used to label the atoms. ZEB−H_2O was thought to be formed through a hydration process catalyzed by CDA. However, the present QM/MM MD study suggests that ZEB−H_2O is unstable in the active site of CDA. A proton transfer from the C_4−OH to Glu-104 occurred during the MD simulations. The K_i value for ZEB−H_2O was estimated to be 1.2×10^{-12} M (ref 24) based on the equilibrium constant for hydration of ZEB in solution (4.7×10^{-6}) and the apparent K_i value observed for ZEB (2.5×10^{-7} M). (C) Possible steps during the binding (hydration) of ZEB. They include the protonation of N_3 of ZEB (from I to II), the nucleophilic attack of the Zn−hydroxide on C_4 (from II to III), and the proton transfer from the C_4−hydroxide of ZEB−H_2O to Glu-104 (from III to IV). The present free energy simulations suggest that these steps are concerted, and the actual process is I → IV, leading to an alkoxide-like TSA at the active site of CDA, as shown in IV (see text).

It has been suggested that the deamination proceeds through a tetrahedral intermediate (formed by the nucleophilic attack by a Zn−hydroxide group on C_4 of cytidine) with ammonia elimination as the major rate-determining step.[25] The solvent deuterium isotope effect indicates that there are probably two proton transfers during the formation of the tetrahedral intermediate.[25] The catalysis depends critically on the presence of Glu-104, and the mutation of Glu-104 to Ala reduces k_{cat} by 10^8-fold.[14]

Zebularine (ZEB; see Figure 1B) binds to CDA, and a near-perfect TSA is produced at the active site of the enzyme during the binding process.[11,12] The interaction of CDA with the TSA inhibitor has become a paradigm in the studies of the tight binding of TSAs by enzymes and the forces responsible for transition-state stabilization during enzyme catalysis.[2−5] The

formation of this TSA is believed to be catalyzed by CDA through a mechanism that is similar to the formation of the tetrahedral intermediate during the CDA-catalyzed reaction.[10] It is thought that the TSA is the zebularine 3,4-hydrate containing a C_4−OH group (ZEB−H_2O; see Figure 1B) that is formed through the hydration of ZEB (i.e., I → II → III in Figure 1C; the I → II step may be concerted with or proceed II → III; see ref 25). The equilibrium constant for hydration of ZEB in solution is approximately 4.7×10^{-6}, and the apparent K_i value observed for ZEB is 2.5×10^{-7} M.[24] On the basis of these data, the K_i value for ZEB−H_2O was estimated to be 1.2×10^{-12} M.[24] Thus, CDA appears to be strongly inhibited by ZEB−H_2O with an affinity that exceeds the affinity for the inhibitor 3,4-dihydrozebularine (DHZ; see Figure 1B), which contains a proton in place of the C_4−OH group of ZEB−H_2O, by a factor of 10^7−10^8.[24] The origin of the large differential binding affinity (estimated to be ca. 10−13 kcal/mol) is still not clear, although it was proposed that the active site interactions involving the C_4−OH group of ZEB−H_2O could make a major contribution.[11]

In this paper, it is predicted from QM/MM molecular dynamics (MD) simulations that ZEB−H_2O is in fact unstable in the active site of CDA; a proton transfer from the C_4−OH to Glu-104 occurs during the energy minimization and MD simulations of the CDA−ZEB−H_2O complex. The QM/MM free energy simulations further suggest that the nucleophilic attack by the Zn−hydroxide group on C_4 follows I → IV in Figure 1C in a single step; that is, it is concerted with two proton transfers from $O_{\epsilon2}$ of Glu-104 to N_3 of ZEB and from the Zn−hydroxide to $O_{\epsilon1}$ of Glu-104. The concerted process of the nucleophilic attack and the second proton transfer to Glu-104 allows the TSA, an alkoxide-like inhibitor (see IV in Figure 1C), to be stabilized through a mechanism that is similar to the transition-state stabilization in general acid−base catalysis.[27,28] The proton-transfer process from the Zn−hydroxide to Glu-104 is also necessary to generate the general acid (Glu-104) for protonating the leaving ammonia during the enzyme catalysis. Thus, CDA seems to be able to use one step of the reaction (e.g., the proton transfer) to catalyze another step (e.g., the nucleophilic attack) to achieve the transition-state stabilization.

Methods

A fast semiempirical density-functional approach (SCC-DFTB),[29] recently implemented in the CHARMM program,[30] was used for QM/MM molecular dynamics and free energy simulations. The SCC-DFTB approach has been extensively tested against high-level quantum mechanical methods for a range of active site models containing Zn.[29] It was found that the SCC-DFTB approach reproduced structural and energetic properties rather reliably.[29] The initial coordinates for the simulations were obtained from the crystal structure of the CDA−TSA complex (1CTU),[11] which have the transition-state analogue at the active site. The TSA inhibitor was initially assumed to be ZEB−H_2O (see Figure 2A) as generally believed (see below). The MD simulations

(26) Frieden, C.; Kurtz, I. C.; Gilbert, H. R. *Biochemistry* **1980**, *19*, 5303−5309.
(27) Schowen, K. B.; Limbach, H. H.; Denisov, G. S.; Schown, R. L. *Biochim. Biophys. Acta* **2000**, *1458*, 43−62.
(28) Jencks, W. P. *Chem. Rev.* **1972**, *72*, 705−718.
(29) Elstner, M.; Cui, Q.; Munih, P.; Kaxiras, E.; Frauenheim, T.; Karplus, M. *J. Comput. Chem.* **2003**, *24*, 565−581.
(30) Brooks, B. R.; Bruccoleri, R. E.; Olafson, B. D.; States, D. J.; Swaminathan, S.; Karplus, M. *J. Comput. Chem.* **1983**, *4*, 187−217.
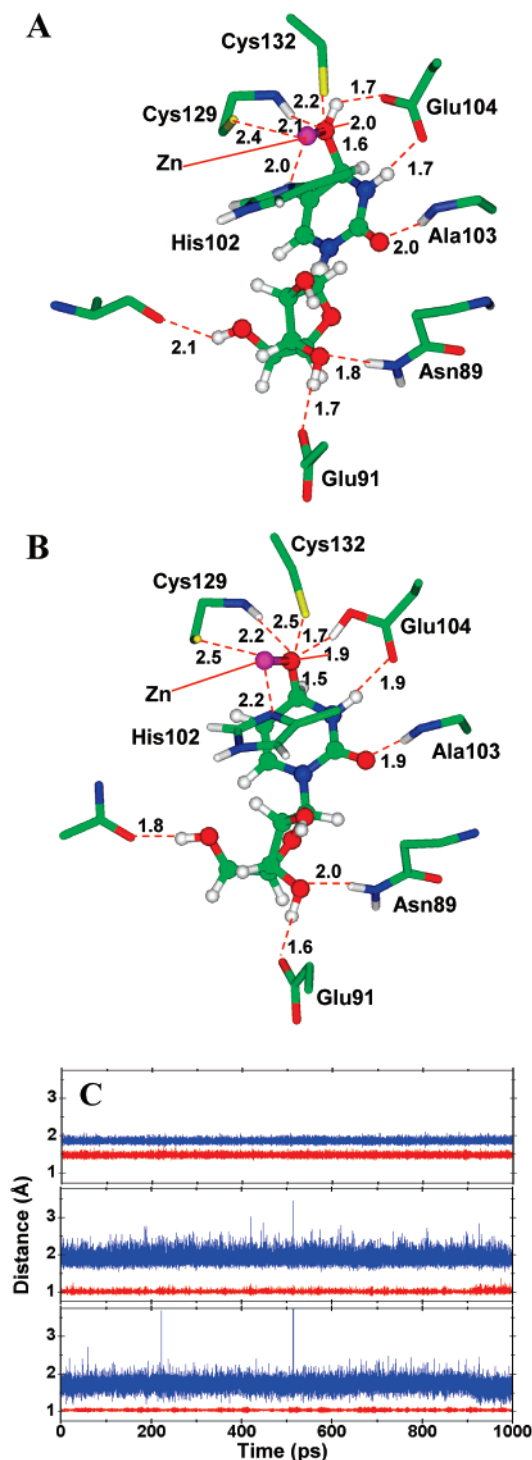
Figure 2. (A) Initial structure generated from the X-ray structure (ref 11) by addition of hydrogen atoms. The inhibitor at the active site is ZEB–H_2O. Distances are in angstroms. (B) Average active-site structure obtained from 1000 frames (50 ps). The further increase of the number of frames has little effect on the structure. A proton transfer from O_4 to Glu-104 has occurred during the energy minimization and MD simulations. (C) Internal motion of the transition-state analogue and its interactions at the active site during the MD simulations monitored by different distances. Top panel: the C_4–O_4 (red) and Zn–O_4 (blue) distances. The C_4–O_4 bond is stable with an average bond distance of 1.5 Å. Middle panel: the N_3–H_3 (red) and $O_{\epsilon2}$ (Glu-104)···H_3 (N_3) (blue) distances. H_3 forms a covalent bond to N_3, and $O_{\epsilon2}$ (Glu-104) accepts a hydrogen bond from N_3–H_3. Bottom panel: the $O_{\epsilon1}$ (Glu-104)–H distance (red) and O_4···H distances. H forms a covalent bond to $O_{\epsilon1}$(Glu-104), and O_4 of ZEB accepts a hydrogen bond from Glu-104.

were performed on the CDA–ZEB–H_2O complex. ZEB–H_2O, Zn, and Glu-104 were treated by QM and the rest of the system by MM. The all-hydrogen potential function (PARAM22)[31] was used for MM atoms. A modified TIP3P water model[32,33] was employed for the solvent. The stochastic boundary molecular dynamics method[34] was used for the QM/MM MD simulations. The system was separated into a reaction zone and a reservoir region, which was deleted; the reaction zone was further divided into the reaction region and the buffer region. The reference point for partitioning the system was chosen as the N_1 atom of ZEB–H_2O (Figure 1B). The reaction region was a sphere with radius 16 Å, and the buffer region has R equal to 16 Å $\leq R \leq$ 18 Å. Inside the reaction region, the atoms were propagated by molecular dynamics, whereas atoms in the buffer region were propagated by Langevin dynamics. The friction constants for the Langevin dynamics were 250 ps^{-1} for the protein atoms and 62 ps^{-1} for the water molecules. A 1 fs time step was used for integration of the equations of motion, and the results of the simulations were saved every 50 fs. In initiating the runs, we performed 500 steps of minimization using the steepest descent method for the protein and solvent atoms. Then minimization was performed for the entire stochastic boundary system with the Adapted Basis Newton Raphson method. The temperature of the system was gradually increased from 50 to 300 K (30 ps) and equilibrated at 300 K (40 ps). The simulations were performed on the resulting systems for several hundred picoseconds to 1 ns.

The initial model system (Figure 2A) generated from the X-ray structure containing ZEB–H_2O was found to be unstable; the proton transfer from O_4 to $O_{\epsilon1}$ of Glu-104 occurred during the QM (SCC-DFTB)/MM energy minimization, leading to a stable alkoxide-like inhibitor at the active site (see Figure 2B and discussions below; the distances from the proton to O_4 and $O_{\epsilon1}$ of Glu-104 are 1.66 and 1.01 Å, respectively). The resulting structure with the alkoxide-like inhibitor was found to be stable during the QM (SCC-DFTB)/MM MD simulations. To further test if this result is meaningful, several other QM/MM approaches were applied, and the initial structure for the inhibitor was also assumed to be ZEB–H_2O with the proton located on O_4 (i.e., the same initial model was used here as that in the case of the SCC-DFTB/MM calculations). The QM methods used in these additional QM/MM calculations include B3LYP/6-31G**,[35a] HF/6-31G**, B97/6-31G**,[35b] HCTH/6-31G**,[35c] and HFEX/6-31G**. Consistent with the results with the SCC-DFTB method, the proton transfer was also observed during the energy minimization with each of these QM/MM methods. The distances from the proton to O_4 ($O_{\epsilon1}$ of Glu-104) were changed from 1 Å (1.7) in the initial structure to 1.53 Å (1.03), 1.75 Å (0.97), 1.56 Å (1.03), 1.60 Å (1.02), and 1.59 Å (0.98) from the B3LYP/6-31G**/MM, HF/6-31G**/MM, B97/6-31G**/MM, HCTH/6-31G**/MM, and HFEX/6-31G**/MM calculations, respectively. The distance between Zn and O_4 obtained from the B3LYP/6-31G**/MM, B97/6-31G**/MM, and HCTH/6-31G**/MM calculations is the same as that from the SCC-DFT/MM calculation (i.e., 1.87–1.88 Å), while the C_4–O_4 distance (1.42 Å) from these calculations is about 0.06 Å shorter. The QM/MM MD and free energy simulations were not performed with these additional QM/MM methods because they are very time-consuming. Thus, the results of the high-level QM/MM energy minimizations support the conclusion that ZEB–H_2O is unstable in the enzyme. In this paper, the alkoxide-like inhibitor in IV of Figures 1C and 2B is designated as the transition-state analogue

(31) MacKerell, A. D., Jr.; Bashford, D.; Bellott, M.; Dunbrack, R. L., Jr.; Evanseck, J. D.; Field, M. J.; Fischer, S.; Gao, J.; Guo, H.; Ha, S.; et al. *J. Phys. Chem. B* **1998**, *102*, 3586–3616.
(32) Jorgensen, W. L. *J. Am. Chem. Soc.* **1981**, *103*, 335–340.
(33) Neria, E.; Fisher, S.; Karplus, M. *J. Chem. Phys.* **1996**, *105*, 1902–1921.
(34) Brooks, C. L., III; Brunger, A.; Karplus, M. *Biopolymers* **1985**, *24*, 843–865.
(35) (a) Lee, C.; Yang, W.; Parr, R. G. *Phys. Rev. B* **1988**, *37*, 785. (b) Becke, A. D. *J. Chem. Phys.* **1997**, *107*, 8554–8560. (c) Hamprecht, F. A.; Cohen, A. J.; Tozer, D. J.; Handy, N. C. *J. Chem. Phys.* **1998**, *109*, 6264–6271. (d) Zhao, Y.; Truhlar, D. G. *J. Phys. Chem. A* **2004**, *108*, 6908–6918.
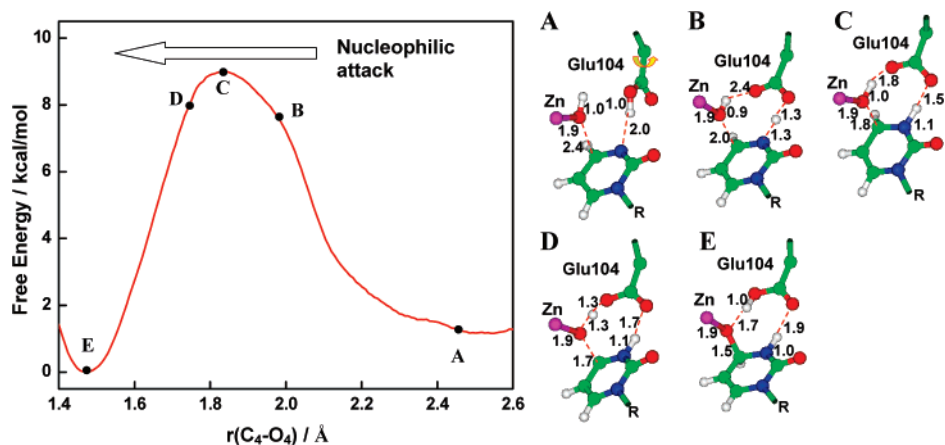
Figure 3. Free energy (potential of mean force) as a function of the C_4-O_4 distance. The average structures at different points (**A**, **B**, **C**, **D**, and **E**) during the nucleophilic attack are given. The structure at **A** is the structure for the CDA−ZEB complex (i.e., before the nucleophilic attack). The structure at **E** is the structure after the nucleophilic attack on C_4 by the Zn−hydroxide. Two proton transfers occur during the nucleophilic attack: one proton transfers from $O_{\epsilon 2}$ of Glu-104 to N_3 and the other transfers from the Zn−hydroxide to $O_{\epsilon 1}$ of Glu-104. The protonation of N_3 by Glu-104 is ahead of the deprotonation of the Zn−hydroxide. The free energy difference between **A** and **E** is ca. 1.5 kcal/mol with the structure at **E** being more stable.

(TSA) to be distinguished from the unstable ZEB−H_2O in III of Figures 1C and 2A.

The umbrella sampling method[36] implemented in the CHARMM program along with the Weighted Histogram Analysis Method (WHAM)[37] was applied to determine the changes of the free energy (potential of mean force) along three reaction coordinates starting from the stable TSA structure obtained from the MD simulations (Figure 2B). The free energy curves were obtained for the processes of the nucleophilic attack of the Zn−hydroxide on C_4 (monitored by the distance between C_4 and O_4), the proton transfer between the Zn−hydroxide and $O_{\epsilon 1}$ of Glu-104 [monitored by $r(O_{\epsilon 1}-H) - r(O_4-H)$], and the deprotonation (protonation) of N_3 by Glu-104 [monitored by $r(N_3-H_3) - r(O_{\epsilon 2}-H_3)$]. It was found that all of the three steps correspond to the same transformation between I and IV in Figure 1C; the three free energy profiles were also found to be similar. Therefore, only the free energy profile for the nucleophilic attack step is reported here. The harmonic umbrella potentials with a force constant of 100−500 kcal mol^{-1} Å^{-2} were used. Twenty windows were used for the nucleophilic attack by the Zn−hydroxide, and 70 ps simulations (20 ps equilibration and 50 ps production run) were performed for each window. To estimate the effect of the proton transfer from the Zn−hydroxide to Glu-104 on the stability of the TSA, the free energy was obtained for the nucleophilic attack step with the O_4−H bond (1.00 Å) fixed by the SHAKE algorithm.[38] As a result, Glu-104 can still protonate N_3 but is unable to accept the proton from O_4.

Results

An important test for the methods of the QM/MM MD simulations is to see if the average structure generated from the simulations agrees with the one determined by X-ray crystallography. In Figure 2B, an average active-site structure based on 1000 frames in the MD trajectory is compared with the initial structure (Figure 2A) generated from the X-ray structure by addition of hydrogen atoms using the CHARMM program.[30,31] As can be seen from Figure 2A,B, the active-site structure of the CDA−TSA complex from the QM/MM simulations is generally close to the initial structure, suggesting the computational approaches used in this study are meaningful.

(36) Torrie, G. M.; Valleau, J. P. *Chem. Phys. Lett.* **1974**, *28*, 578−581.
(37) Kumar, M.; Bouzida, D.; Swendsen, R. H.; Kollman, P. A.; Rosenberg, J. M. *J. Comput. Chem.* **1992**, *13*, 1011−1021.
(38) Ryckaert, J. P.; Ciccotti, G.; Berendsen, H. J. C. *J. Comput. Phys.* **1977**, *23*, 327−341.

However, there is a major difference in these two structures. For the initial structure in Figure 2A, the inhibitor was assumed to exist as ZEB−H_2O.[3−5] This is in contrast with the average structure in Figure 2B, where the proton on O_4 has already transferred to $O_{\epsilon 1}$ of Glu-104 during the energy minimization and remained on $O_{\epsilon 1}$ during the QM/MM MD simulations. Thus, the QM/MM results suggest that the structure of the CDA−ZEB−H_2O complex is likely to be unstable, and the transition-state analogue may exist as an alkoxide-like inhibitor at the active site (see Figure 2B). This suggestion is supported by the additional QM/MM calculations (see Methods).

The CDA−ZEB−H_2O complex has been the subject of a previous QM/MM MD study,[23] where Glu-104 was not treated by the QM method. As a result, Glu-104 was unable to accept a proton from O_4 or N_3, and the CDA−ZEB−H_2O complex could not change to the CDA−TSA complex or the CDA−ZEB complex. It was found that the C_4−O_4 bond of ZEB−H_2O underwent transient bond breaking and making during the MD simulations;[23] the reason for this instability was not clear at the time. In Figure 2C, the internal motion of the stable alkoxide-like transition-state analogue and its interactions with the active-site groups during the MD simulations are monitored using the C_4−O_4, Zn−O_4, N_3−H_3, $O_{\epsilon 2}$ (Glu-104)···H_3 (N_3), $O_{\epsilon 1}$ (Glu-104)−H, and O_4···H (Glu-104) distances. Consistent with the structure in Figure 2B, Glu-104 is protonated with the $O_{\epsilon 1}$−H distance of ca. 1 Å (bottom panel, red). Moreover, the C_4−O_4 bond (top panel, red) is now stable without the transient bond breaking and making observed in the earlier study.[23] Thus, the previous observation of the transient bond breaking and making is due to the assumption that there exists a stable ZEB−H_2O at the active site. The results of the present simulations suggest that this assumption in the crystallographic least-squares refinement needs to be re-examined as well.

The change of free energy (potential of mean force) as a function of the C_4−O_4 distance is plotted in Figure 3; five average structures along the free energy curve are also given for the groups involved, representing different stages of the nucleophilic attack by the Zn−hydroxide on C_4. The average structure at **A** corresponds to the CDA−ZEB complex with a C_4−O_4 distance of about 2.4 Å. The QM/MM MD simulations

were also performed for this complex for 500 ps without the harmonic umbrella potentials. The CDA−ZEB complex was found to be stable, and the proton transfer from $O_{\epsilon 2}$ of Glu-104 to N_3 did not occur during the simulations. It appears that this proton transfer could occur only when the structure of ZEB is significantly perturbed by the nucleophilic attack with a partial sp^2 to sp^3 rehybridization of N_3.[25]

Consistent with an earlier linear-scaling quantum mechanical investigation,[20,21] $Zn−OH^-$ exists as the active species before the nucleophilic attack from the simulations. It has been suggested earlier[25] based on solvent deuterium isotopic effects that the proton from $Zn−H_2O$ does not transfer to Glu-104 before the substrate and, presumably, inhibitor binding. To examine whether the simulations could lead to the same conclusion, a model for CDA without the inhibitor was built and 500 ps QM/MM MD simulations were performed. The initial structure in Figure 2A was used as a starting structure, and ZEB−H_2O was simply replaced by H_2O; this water molecule was treated by QM along with Zn and Glu-104. Consistent with the experimental suggestion, the protons on Zn−H_2O were found to be stable and did not transfer to Glu-104, even though one of the protons was hydrogen-bonded to $O_{\epsilon 1}$ of Glu-104 throughout the simulations. Thus, the pK_a value of Glu-104 may be elevated due to the ZEB binding. High pK_a values (about 8−10) for the carboxyl group have been proposed for other enzymes (see refs 39 and 40).

As the nucleophilic attack proceeds to **B** with $r(C_4−O_4) =$ 2.0 Å, the average position of the proton (H_3) moves to the center between $O_{\epsilon 2}$ and N_3; the $N_3···O_{\epsilon 2}$ distance is around 2.6 Å (see the average structure at **B** in Figure 3). As it will be shown later, H_3 actually moves back and forth between $O_{\epsilon 2}$ and N_3 on a picoseconds scale. $O_{\epsilon 1}$ of Glu-104 now forms a hydrogen bond with the Zn−hydroxide. At the transition state (**C**), N_3 has already been protonated by Glu-104, while the second proton transfer from the Zn−hydroxide to $O_{\epsilon 1}$ has not started yet. The second proton transfer occurs as the nucleophilic attack on C_4 proceeds further along the reaction coordinate (see the structures at **D** and **E**). Thus, the simulations suggest that protonation of N_3 by Glu-104 is ahead of deprotonation of the Zn−hydroxide. Moreover, they indicate that the pK_a value of the Zn−hydroxide may be significantly depressed in the enzyme as a result of the $C_4−O_4$ bond formation. Although the locations of the two protons at **C** are similar to those in the ZEB−H_2O complex shown in Figure 2A, the $C_4−O_4$ bond is not formed; the average distance between the C_4 and O_4 atoms at **C** is about 1.8 Å. Figure 3 shows that the free energy difference between **A** and **E** (i.e., before and after the nucleophilic attack) is ca. 1.5 kcal/mol from the simulation; the CDA−TSA complex (**E**) is more stable than the CDA−substrate analogue complex (**A**). The free energy barrier from **A** to **E** was calculated to be about 8 kcal/mol.

The dynamics of the protons at **B** and **D** are monitored in Figure 4A,B, respectively; $r(N_3−H_3)$ and $r(O_{\epsilon 2}−H_3)$ are used to monitor the motion of H_3, whereas $r(O_4−H)$ and $r(O_{\epsilon 1}−H)$ are used to monitor the motion of H. It is interesting to note from Figure 4A (top panel) that the proton (H_3) involved in the protonation of N_3 moves back and forth on a picoseconds scale

(39) Deng, H.; Callender, R.; Zhu, J.; Nguyen, K. T.; Pei, D. *Biochemistry* **2002**, *41*, 10563−10569.
(40) Ma, J.; Zheng, X.; Schnappauf, G.; Braus, G.; Karplus, M.; Lipscomb, W. N. *Proc. Natl. Acad. Sci. U.S.A.* **1998**, *95*, 14640−14645.
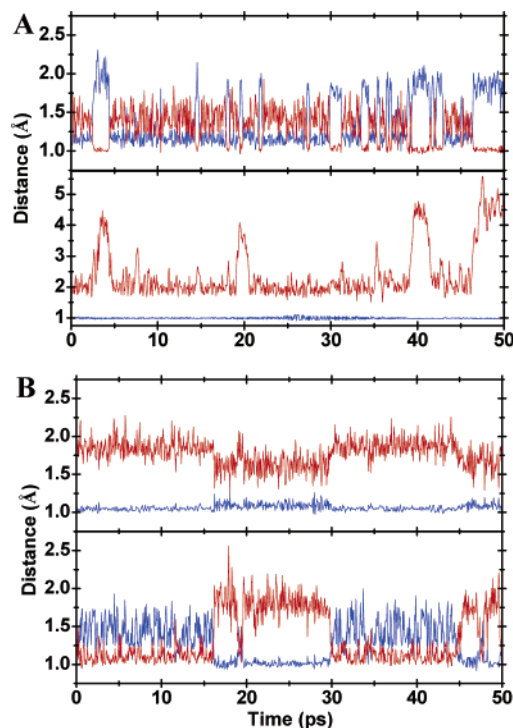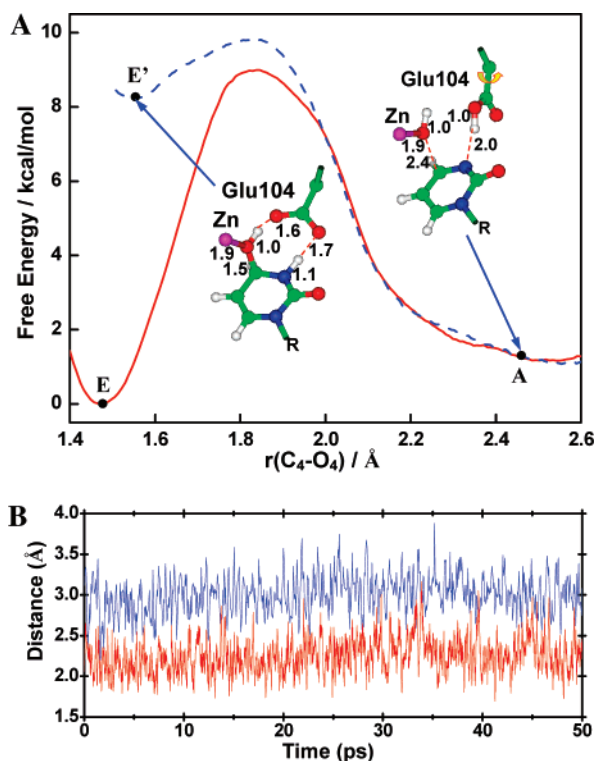
Figure 4. (A) Typical fluctuations of the covalent bond and hydrogen bond distances at **B** on the free energy curve in Figure 3. Top panel: $r(N_3−H_3)$ (blue) and $r(O_{\epsilon 2}−H_3)$ (red). The proton (H_3) moves back and forth between N_3 and $O_{\epsilon 2}$ with the average position in the middle of the two atoms (see the structure at **B** in Figure 3). Bottom panel: $r(O_4−H)$ (blue) and $r(O_{\epsilon 1}−H)$ (red). The proton is on O_4 with a bond distance of 1 Å. $O_{\epsilon 1}$ accepts a hydrogen bond from $O_4−H$. (B) Typical fluctuations of the covalent bond and hydrogen bond distances at **D** of the free energy curve in Figure 3. Top panel: $r(N_3−H_3)$ (blue) and $r(O_{\epsilon 2}−H_3)$ (red). The proton is on N_3 with a bond distance of 1 Å. $O_{\epsilon 2}$ accepts a hydrogen bond from $N_3−H_3$. Bottom panel: $r(O_4−H)$ (blue) and $r(O_{\epsilon 1}−H)$ (red). The proton moves back and forth between O_4 and $O_{\epsilon 1}$ of Glu-104 with the average position in the middle of the two atoms (see the structure at **D** in Figure 3).

between N_3 and $O_{\epsilon 2}$ at **B** (as indicated by the changes of the $N_3−H_3$ and $O_{\epsilon 2}−H_3$ distances), even though its average position is in the middle of the two atoms. Thus, the proton of the $N_3···H_3−O_{\epsilon 2}$ hydrogen bond spends most of the time near either N_3 or $O_{\epsilon 2}$ with a distance that is close to the one for a covalent bond (e.g., 1.0−1.15 Å). However, the corresponding bond-distance fluctuation is generally greater than those involving normal covalent bonds. This can be seen by comparing the fluctuations for the $N_3−H_3$ distance in Figure 4A (top panel, blue line) and 4B (top panel, blue line) where the fluctuation in the former case is more significant. This observation might be applied to some of the low-barrier hydrogen bonds widely observed in biological structures. Figure 4B (top panel) shows that the protonation of N_3 has already completed at **D** with a $N_3−H_3$ bond distance at about 1 Å (blue line). Figure 4B (bottom panel) shows that the second proton moves back and forth between O_4 and $O_{\epsilon 1}$ of Glu-104 when the nucleophilic attack reaches **D**; the average position of the proton is also located in the middle of the two oxygen atoms involved in the interaction (see structure **D** in Figure 3). This second proton transfer to $O_{\epsilon 1}$ of Glu-104 is completed when the nucleophilic attack proceeds further to **E** (see Figure 2B,C for the corresponding structural and dynamic information at **E**). Comparison of the fluctuations for $r(O_{\epsilon 1}−H)$ in Figure 4B (bottom panel, red line) and Figure 2C (bottom panel, red line) shows that the

Figure 5. (A) Comparison of the free energies as functions of the C_4-O_4 distance with and without the constraint on the O_4-H bond. Red (solid line): without the constraint on the O_4-H bond (same as in Figure 3). Blue (dashed line): with the constraint on the O_4-H bond to prevent the proton transfer away from O_4. Comparison of the two curves shows that the proton transfer from O_4 to $O_{\epsilon1}$ of Glu-104 along with the possible strengthening of the interaction between the TSA and enzyme may make a very important contribution to the stability of the TSA (ca. 8 kcal/mol). (B) Fluctuations for the distance between $H-N$ (Cys-129) and O_4 as a function of the time at **E** (red) and **E'** (blue), respectively. A hydrogen bond is formed between the backbone $N-H$ group of Cys-129 and O_4 at **E** with an average $(N)H{\cdots}O_4$ hydrogen bond distance of 2.2 Å. This hydrogen bond cannot be formed at **E'** containing ZEB$-H_2O$ (i.e., obtained with the assumption that the proton H is located at O_4); the average distance is about 3 Å.

fluctuation for the $O_{\epsilon1}-H$ bond at **D** is also greater than that at the stable CDA$-$TSA conformation (**E**).

To estimate the effect of the second proton transfer from the Zn$-$hydroxide to Glu-104 on the stability of the alkoxide-like TSA at the active site, the O_4-H bond was fixed at 1.00 Å using the SHAKE algorithm.[37] As a result, Glu-104 can still protonate N_3 but is unable to accept the proton from O_4. The free energy as a function of the C_4-O_4 distance was then determined using the same procedure. The two free energy curves obtained with and without the constraint on the O_4-H bond are compared in Figure 5A. As can be seen from Figure 5A, the shapes of the two free energy curves are essentially the same in the area of $r(C_4-O_4) \geq 2$ Å. This result is expected as the O_4-H bond is intact in the early stage of the nucleophilic attack and the corresponding structures along the reaction coordinate in the two cases are similar. As is evident from Figure 5A, the free energy after the nucleophilic attack is as much as 8 kcal/mol higher for the curve with the constraint (i.e., at **E'**) than that without (i.e., at **E**). One major difference for the two free energy simulations is that the ligand in the CDA complex at **E'** is ZEB$-H_2O$ (the structure is similar to the one in Figure 2A), while it is the alkoxide-like TSA at **E** (Figure 2B). Thus, a major stabilization of the alkoxide-like TSA complex in the

active site seems to rise from the proton transfer from the Zn$-$hydroxide to Glu-104 in the later stage of the nucleophilic attack (i.e., after the transition state).

The alkoxide-like TSA seems to lead to a stronger interaction with the enzyme than ZEB$-H_2O$. Indeed, as can be seen from Figure 5B, the hydrogen bond between the amide group of Cys-129 and O_4 cannot be formed in the CDA$-$ZEB$-H_2O$ complex (**E'**) during the MD simulations; the average distance between H(N) and O_4 is about 3 Å. A similar observation was made in the earlier study.[23] By contrast, a stable hydrogen bond between the amide group of Cys-129 and O_4 can be formed in the CDA$-$TSA complex with an average hydrogen bond distance of 2.2 Å. The formation of this hydrogen bond is likely to make additional contribution to stabilize the alkoxide-like TSA in the active site. Figure 5A shows that ZEB$-H_2O$ at **E'** is more stable by ~2 kcal/mol than the structure at the transition state for the case with the constraint, presumably due to the stronger interactions at the active site as a result of the C_4-O_4 bond formation.[23] Nevertheless, this effect of hydrogen bonding is much smaller than the effect of the proton transfer involving the O_4-H group and Glu-104.

Discussion

Although the binding of ZEB results in a near-perfect TSA at the active site of CDA,[11,12] the origin of the high binding affinity for this inhibitor is still not clear. It is believed that the TSA is zebularine 3,4-hydrate containing a C_4-OH group (ZEB$-H_2O$; see Figure 1B) that is formed through the hydration of ZEB at the active site. Comparison of the structures of CDA complexed with different inhibitors has led to the suggestion that the active-site interactions involving the C_4-OH group of ZEB$-H_2O$ may make a major contribution to the high binding affinity.[11] However, the proton on the C_4-OH group is invisible in the X-ray structure, and the possibility that it may be located on Glu-104 cannot be simply ruled out. Indeed, the present QM/MM MD simulations showed that ZEB$-H_2O$ is in fact unstable in the active site of CDA. A proton transfer from the C_4-OH to Glu-104 occurred during the energy minimizations, and the resulting structure was stable during the QM/MM MD simulations. This proton-transfer process leads to the formation of a stable alkoxide-like TSA (or simply TSA) at the active site (see IV in Figures 1C and 2B) which may not be distinguishable from ZEB$-H_2O$ in the X-ray structure. The average structure of the CDA$-$alkoxide-like TSA complex obtained from the simulations is generally closer to the X-ray structure than the average structure of the CDA$-$ZEB$-H_2O$ complex at **E'** in Figure 5A (except for the location of H), supporting the existence of the TSA, rather than the unstable ZEB$-H_2O$, at the active site. For instance, the X-ray structure showed that there is a hydrogen bond between the backbone $N-H$ group of Cys-129 and O_4.[11] The simulations, however, suggested that whereas this hydrogen bond is stable in the TSA complex, it could not be formed for the ZEB$-H_2O$ complex (Figure 5B), due to the poor geometries for the formation of the two hydrogen bonds between the O_4-H group and $O_{\epsilon1}$ and between the $N-H$ group of Cys-129 and the electron lone-pairs of O_4 simultaneously.

The QM/MM free energy simulations were used to understand the mechanism of the inhibitor binding and the energetic origin of the high binding affinity of the TSA. It was shown that the

nucleophilic attack by the Zn−hydroxide group on C_4 was concerted with two proton-transfer processes from $O_{\epsilon 2}$ of Glu-104 to N_3 of ZEB and from the Zn−hydroxide to $O_{\epsilon 1}$ of Glu-104, leading to the alkoxide-like TSA (i.e., I → IV, Figure 1C). The protonation of N_3 by Glu-104 was found to be completed before the nucleophilic attack reaches the transition state, while deprotonation of the Zn−hydroxide started mainly after the transition state was reached (see Figure 3). No stable ZEB−H_2O was observed during the free energy simulations, supporting the conclusion from the MD simulations that this species is unstable at the active site (see above). The results reported here seem to be consistent with the previous study of ^{15}N isotope effects on CDA-catalyzed deamination of cytidine,[25] which proposed that two or more protons were transferred during the formation of the tetrahedral intermediate. However, the existence of the alkoxide-like TSA in the active site and the absence of a stable ZEB−H_2O from the simulations indicate that the tetrahedral intermediate formed during the enzyme catalysis might be alkoxide-like as well, resembling a second tetrahedral intermediate proposed earlier,[12] although a detailed study is still necessary.

The equilibrium constant for hydration of ZEB to generate ZEB−H_2O in solution was estimated to be approximately 4.7 × 10^{-6},[24] and the equilibrium constant for generating the corresponding alkoxide-like compound is probably even lower. Figure 3 shows that the CDA−TSA complex (**E**) is about 1.5 kcal/mol more stable than the CDA−ZEB complex (**A**) based on the free energy simulations. Thus, the enzyme is able to reduce the instability (or increase the stability) of the TSA relative to ZEB by at least 9 kcal/mol compared to the case in solution. This effect is close to the previous estimate (about 10 kcal/mol) based on experimental data.[3,5,11,24] However, the nucleophilic attack of the Zn−hydroxide on C_4 did not lead to ZEB−H_2O from our study, and the stabilization of the TSA cannot be simply attributed to the interactions involving the C_4−OH group, as proposed previously. Indeed, when the O_4−H covalent bond was fixed by SHAKE in the free energy simulations (see Figure 5A, blue dashed line), the resulting CDA−ZEB−H_2O complex (i.e., at **E′** in Figure 5A) was found to be as much as 6−7 kcal/mol less stable than the CDA−ZEB complex (i.e., at **A** in Figure 5A). Thus, the proton transfer from

Zn−hydroxide to Glu-104 along with the possible strengthening of the interaction involving the TSA (see above) may provide a stabilizing effect of about 8 kcal/mol for the CDA−TSA complex. This effect is much greater than the effect of the hypothetical hydrogen-bonding interaction involving the C_4 hydroxyl group of ZEB−H_2O, which was estimated to be only about 2 kcal/mol (Figure 5A).

Conclusions

The QM/MM MD and free energy simulations have been performed on CDA to understand the inhibitor binding and the origin of the high binding affinity for TSA. Zebularine 3,4-hydrate was found to be unstable at the active site of CDA from the simulations. It was suggested that the nucleophilic attack by the Zn−hydroxide group on C_4 is concerted with two proton-transfer processes, leading to the formation of a stable alkoxide-like TSA at the active site. Such concerted process allows the TSA to be stabilized through a mechanism that is similar to the transition-state stabilization in general acid−base catalysis.[27,28] The proton transfer from the Zn−hydroxide to Glu-104 is necessary to generate the general acid (Glu-104) for protonating the leaving ammonia during the enzyme catalysis. Thus, CDA seems to be able to use this proton transfer to stabilize the alkoxide-like tetrahedral intermediate[26] and therefore achieve transition-state stabilization. The results may have important implications for some other zinc enzymes as well, where a proton transfer involving a Glu or Asp residue interacting with a Zn-activated hydroxide nucleophile could play an important role during the catalysis.[10,41]

JA0439625

(41) Christianson, D. W.; Cox, J. D. *Annu. Rev. Biochem.* **1999**, *68*, 33−57.